Journal of Materials Chemistry

Cite this: J. Mater. Chem., 2011, 21, 2369

www.rsc.org/materials

PAPER

Flower-shaped PdI_2 nanomaterials with remarkable surface-enhanced Raman scattering activity†

Lianmeng Wang,[a] Lihua Wang,[b] Enzhong Tan,[a] Lidong Li,[a] Lin Guo*[a] and Xiaodong Han*[b]

Received 10th August 2010, Accepted 1st November 2010
DOI: 10.1039/c0jm02610g

Uniform dispersed flower-shaped palladium iodide (PdI_2) nanoparticles were prepared successfully by a simple wet chemical method. The as-synthesized products were structurally and morphologically characterized by X-ray diffraction (XRD), scanning electron microscopy (SEM), transmission electron microscopy (TEM), as well as high resolution transmission electron microscopy (HRTEM). Large numbers of twin and stacking faults were observed at the tip of the petals of flower-shaped morphology. At the same time, a series of palladium iodide structures with different morphology and size were obtained through the manipulation of the concentration of KI and the reaction temperature. The formation of typical flower-shaped palladium iodide was correlated with their reaction conditions. The as-produced PdI_2 nanoparticles exhibit high surface-enhanced Raman scattering (SERS) activities for malachite green (MG) probe molecules with 1.0×10^{-7} M concentration. As a result, the flower-shaped PdI_2 nanostructures coupled with SERS hold a great potential as a rapid and ultra-sensitive agent for detecting trace amounts of prohibited substances in contaminated food samples.

1. Introduction

Palladium nanomaterials have attracted much interest due to their extraordinary catalytic properties, for reactions such as the Suzuki, Heck, Stille and Sonogashira coupling-reactions.[1–3] They can also serve as potential hydrogen sensors and hydrogen storage material,[4–6] powerful pollutant eliminating agents in automobile applications (CO and NO),[7] potential substrates for surface enhanced Raman scattering based on surface plasmon resonance peaks (SPR),[8,9] excellent electrocatalysts for ethanol electrooxidation in alkaline media in direct ethanol fuel cells,[10] future application in spintronic technology owing to their existing magnetism,[11] and biosensors.[12] In recent years, lots of methods have been adopted to synthesise single elemental palladium nanomaterial.[13–17]

In the mean time, with a much lower cost, different palladium salts, coordination compounds and proper reagents could also achieve the same catalytic effect compared with the noble metals (single matter). For example, a palladium acetate and DMSO system and a palladium iodide and KI system were successfully used to obtain the target product in an organic reaction.[18–20] Accordingly, adopting proper synthetic methods for obtaining novel morphologies and functions of nano palladium salts and coordination compounds is urgently required. Here, we prepared nearly uniformly-dispersed flower-shaped palladium iodide nanomaterials by a simple wet chemical method in high yield. With the special flower-shaped morphology, the nano palladium iodide was made as the substrate for surface-enhanced Raman scattering (SERS) with remarkable signals. The nano palladium iodide could be a potential candidate to replace the pure palladium nanomaterials at particular detecting fields which will save valuable energy resources.

2. Experiment section

2.1 Materials

Ethylene glycol (Beijing chemical factory, 500 mL), palladium(II) acetate (J&KCHEMICA, 234582, 10 g), potassium iodide (Tianjin chemical factory, 500 g), and hydrochloric acid (Beijing chemical factory, 500 mL) were all analytical grade purity and were used without further purification.

2.2 Instrumentation

X-ray diffraction (XRD) pattern of the product was carried out on a Rigaku, Dmax2200 diffractometer equipped with a Cu Kα radiation source (λ = 1.54180 Å) for the structural determination. Further microstructural analyses were performed by using a Hitachi S4800 cold field emission scanning electron microscope (CFESEM) and a high resolution transmission electron microscope (HRTEM) (JEOL 2010F). TEM samples were prepared by diluting the resulting solution with alcohol by ultrasonic

[a]School of Chemistry and Environment, Beijing University of Aeronautics and Astronautics, Beijing, China 100191. E-mail: guolin@buaa.edu.cn; Tel: +86-10-82338162
[b]Institute of Microstructure and Properties of Advanced Materials, Beijing University of Technology, Beijing, China 100022. E-mail: xdhan@bjut.edu.cn; Tel: +86-10- 67392281

† Electronic supplementary information (ESI) available: SEM images of prepared PdI_2 at different quantities of KI. See DOI: 10.1039/c0jm02610g

treatment, and dropping it onto a holey carbon film supported on a copper grid, and drying the dropped sample in air. Thermogravimetric analysis (TGA) for heating the as-prepared flower-shaped nano palladium iodide was conducted by using a Perkin-Elmer Diamond TG-DTA system (N_2 protected at a rate of 10 mL s^{-1}). SERS substrates were fabricated by dropping the PdI_2 ethanol solution onto a Si wafer and drying completely under vacuum. The dry films were immersed in a different concentration aqueous solution of MG for 0.5 h in order to absorb enough probe molecules. The substrate was then taken out, rinsed with deionized water to remove any unabsorbed MG molecules and dried with a stream of air. Raman spectra were recorded with a JY LabRAM HR800 UV confocal micro-Raman spectrometer. The He–Ne laser (632.8 nm) was used as a source of excitation, the laser radiation was focused on the sample by means of a 100× microscope objective. The signal acquisition time was 10 s.

2.3 Synthesis of flower-shaped palladium iodide

In a typical synthesis of flower-shaped palladium iodide, 0.083 g of KI (0.5 mmol) was first put into the bottom of a 50 mL three-necked flask (equipped with a reflux condenser and a magnetic Teflon-coated stirring bar), and then 25 mL of ethylene glycol (EG) was added by intensive stirring to obtain a homogeneous transparent solution at 60 °C. The whole solution was kept under stirring for an hour. At the same time, 0.0112 g of palladium acetate (0.5 mmol) was dissolved in the mixture of 1.6 mLof HCl (0.24 M) and 3.4 mLof EG in a small beaker, the palladium acetate solution was poured into the flask quickly under vigorous stirring. The color of the solution turned from colorless to black immediately, indicating palladium iodide nanoparticle formation. The whole solution was then kept under stirring for another 30 min. The temperature was raised to 130 °C and held at this temperature for 3 h in order to complete the reaction, the product was collected by centrifugation at low speed (8000 rpm), followed by washing several times with ethanol and pure water. Eventually, the precipitate product was redispersed in ethanol.

3. Results and discussion

3.1 Characterization of flower-shaped Palladium iodide

The XRD spectrum for the flower-shaped PdI_2 was shown in Fig. 1. All of the diffraction peaks matched well with Bragg reflections of the standard monoclinic crystal structure with space group: P21/C and lattice parameters of $a = 0.6690$, $b = 0.8600$ nm, $c = 0.6870$ nm, $\beta = 103.50°$ (JCPDF # 73-2474). The subsequent high resolution electron microscopy (HRTEM) analysis supported these X-ray diffraction results. The thermogravimetric analysis was then used to confirm the purity of the as-synthesized palladium iodide. As can be revealed from Fig. 2, the thermo-gravimetric curve of the product (under protection by a N_2 atmosphere) showed that the weight-losing started at about 300 °C [lower than the bulk materials (350 °C)] and ended at 500 °C. The experimental results (31%) agree with the theoretic values (30%, $PdI_2 \rightarrow Pd$) very well and this indicated that the final product was pure palladium. The weight of the final product

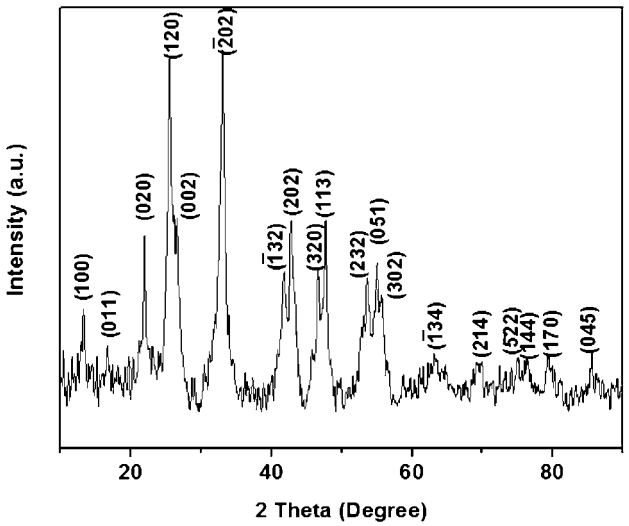

Fig. 1 XRD pattern of the as-synthesized flower-shaped palladium iodide, all of the peaks can be indexed to pure phase with a monoclinic structure.

didn't change after 500 °C and this indicated the oxidation of palladium didn't occur.

Scanning electron microscopy images of the as-produced PdI_2 products are shown in Fig. 3a. It can be clearly seen that the products were relatively uniform flower-shaped nano-architectures with a diameter of around 400 nm. From the amplified image of flower-shaped PdI_2 nanoparticles (Fig. 3b), large numbers of irregular petals can be recognized. The crystallography characters and the chemical composition of the as-synthesized PdI_2 nanoparticles were further investigated by transmission electron microscopy (TEM) and energy dispersive X-ray spectroscopy (EDS). Fig. 4a shows a low-magnification TEM image of the nano flower-shaped PdI_2 particles. The as-synthesized PdI_2 nanoparticles possess high mono-dispersivity and with an average size of about 400 nm. The EDS spectrum (inset, Fig. 4b) idicates that the nanoparticles contained the Pd and I elements in an atomic ratio close to 1 : 2 and which is consistent with the results of Fig. 1. The Cu element in the EDS spectrum came from the TEM grid. Fig. 4b was the magnified TEM image taken from the red framed region of Fig. 4a and it

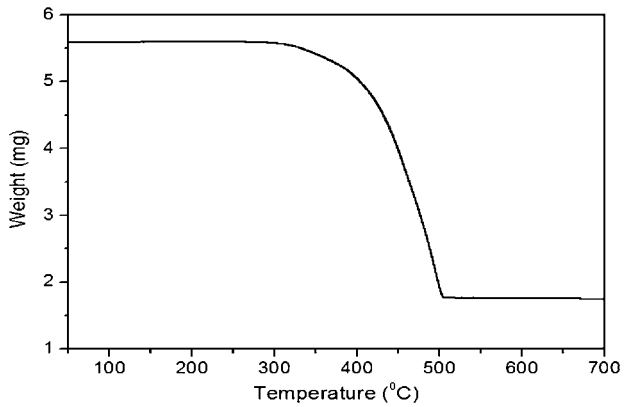

Fig. 2 Thermo-gravimetric curve of the flower-shaped palladium iodide.

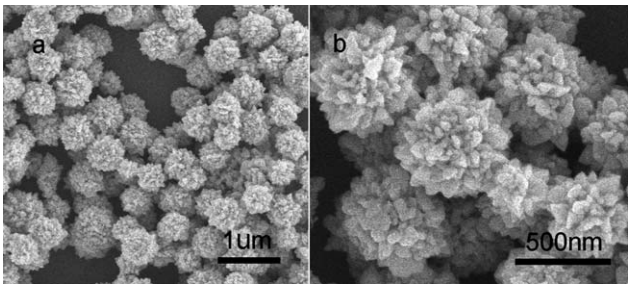

Fig. 3 SEM images of the as-synthesized flower-shaped palladium iodide with different magnification.

presented a typical flower-like architecture with radial-distributed petals. These radial-distributed petals grew surrounding a center-core with diameter of about 300 nm. These petals were about 150 nm in length and 80 nm in width. Fig. 4c is a HRTEM image recorded along the [010] direction which was taken from the red framed region (marked with 'c') of Fig. 4b. The lattice fringe spacings marked with 0.41 nm and 0.64 nm corresponded to the (020) and (100) crystal planes of the monoclinic structure of PdI_2. These "flower petals" grow along the [110] direction as indicated by the white arrows and with the side facets of (100) and (010) planes. The twin boundaries were indicated by white lines in Fig. 4c. The stacking faults were also marked with red lines in the same figure. Fig. 4d was the selected-area electron diffraction (SAED) pattern. The set of rings can be indexed as the monoclinic structured PdI_2 and is consistent with the XRD result in Fig. 1. Fig. 4e shows an HRTEM image of another petal. The fast Fourier transformation pattern (inset, Fig. 4e) shows the obvious twin diffraction patterns. The diffraction spots can again be indexed by the monoclinic structure.[21] Fig. 4f was the enlarged image taken from the white framed region of Fig. 4e. The two-dimensional projected atomic structural model and the corresponding simulated HRTEM images (overlaid in Fig. 4f) agreed well with the experimental recorded HRTEM images of the monoclinic structure. Large numbers of petals were studied and it was revealed that most of the petals grew in a radial way from the nanoflower center and with their [110] direction pointing outside as shown in Fig. 5a. The corresponding high magnified

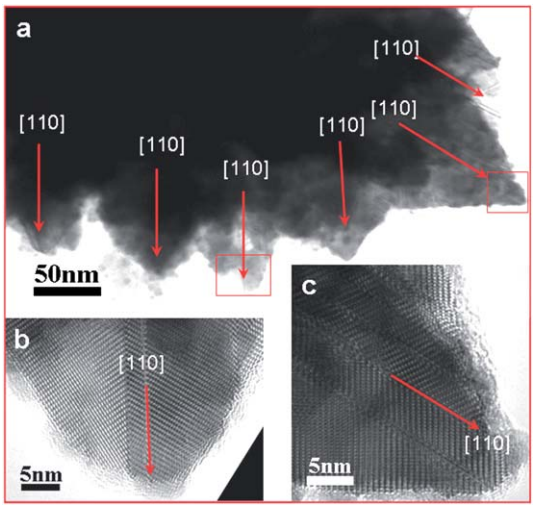

Fig. 5 TEM images of prepared PdI_2 and preferential crystal growth direction.

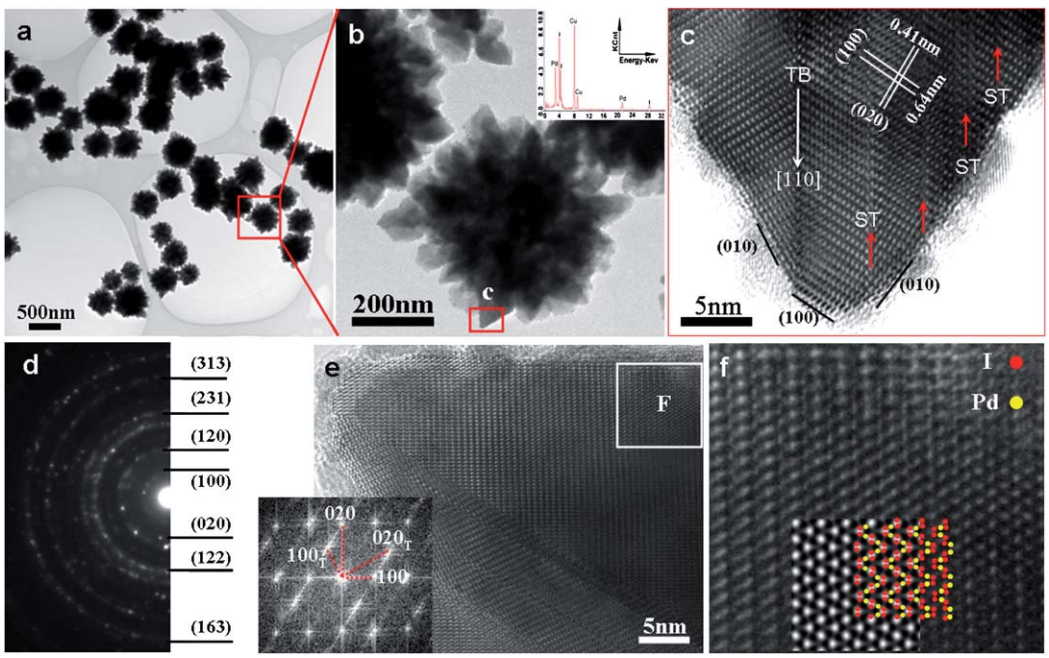

Fig. 4 TEM images of the as-synthesized flower-shaped PdI_2 with different magnification (a–b), and an HRTEM image of the product selected from (b) (marked as 'c') is shown in (c), the insets are the corresponding EDS images of the flower-shaped PdI_2. (d) Corresponding SAED pattern. (e) HRTEM image of another petal, the inset is the corresponding fast Fourier transformation patterns of (e). (f) Enlarged HRTEM image taken from the framed region in (e), two dimensional projected atomic structural models and the simulated HRTEM images of the perfect crystalline lattices are shown as insets.

HRTEM images (Fig. 5b and Fig. 5c) show the [110] orientation of the flower-petals clearly.

3.2 Influence of experimental conditions

The morphology and size of nanostructured materials can be affected by different factors such as the temperature, velocity of adding reactant and the quantity of precursors *etc.* Here, we first evaluated the impact of the quantity of KI. It was revealed that the output of the product decreased sharply with increasing the quantity of KI. When the quantity of KI reached 0.9 mmol, the product couldn't be separated from the solution, and the solution was homogeneous and aubergine in colour. This result was caused by the complete dissolution of the as-synthesized PdI_2 nanomaterials in excess KI solution. The morphologies of the product can also be affected by controlling the amount of KI (Fig. S1, ESI†). Consequently, an optimal amount of KI was necessary for achieving the desired flower-shaped PdI_2 morphology. Another influential factor in our experiment was the temperature at the initial stage. With the initial temperature being set up at 60 °C, 70 °C and 80 °C, respectively, as shown in Fig. 3 and Fig. 6, the final morphology of the product was unchanged in this small temperature range, but exhibited a great change in size. For example, the ultimate size of PdI_2 nanoparticles was about 400 nm if the initial temperature was 60 °C (see Fig. 3, typical synthesis procedure), but it decreased to 200 nm for 70 °C (see Fig. 6a). After the initial temperature increased to 80 °C (see Fig. 6b), the size of the PdI_2 nanoparticles exhibited poor mono-dispersivity with a size range of 200–500 nm. At higher than or equal to 90 °C, both the flower-shaped architecture morphology and the mono-dispersivity were destroyed (see Fig. 6c and Fig. 6d). We thus demonstrated that the quantity of KI and the initial temperature were key factors for tuning the size and morphologies of PdI_2 nanoparticles and for achieving flower-shaped PdI_2 nanomaterials in high yield. With regard to detailed information for the formation procedure of flower-shaped morphology in a typical synthetic route see Fig. S2 (ESI†).

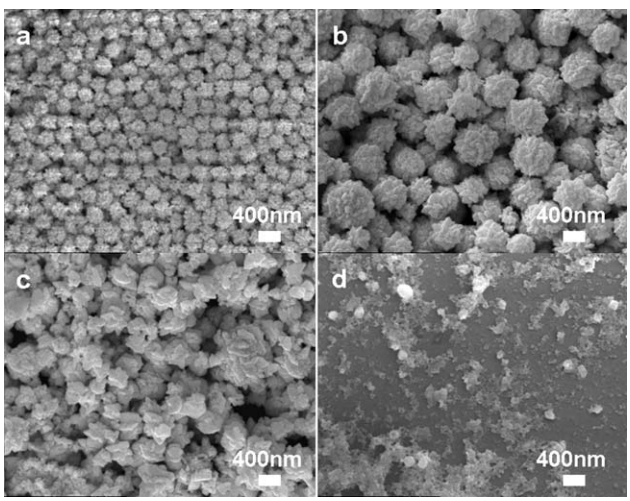

Fig. 6 SEM images of prepared PdI_2 at different temperature, (a) 70 °C, (b) 80 °C, (c) 90 °C, (d) 100 °C.

3.3 Surface-enhanced Raman scattering detection of palladium iodide

Surface-enhanced Raman scattering has been a powerful tool for optical detection and for spectroscopic investigation of single molecules absorbed on nanostructural substrates. It can meet the urgent requirement of detecting trace prohibited substances and probe molecules in many areas. Nowadays, it is generally accepted that there are two mechanisms which explain the overall SERS effect: the charge-transfer (CT) mechanism and the electromagnetic (EM) mechanism. SERS active substrates include some noble metals and transitional metals, for which the major enhancement mechanism occurs through electromagnetic enhancement.[22,23] In the very few studies of SERS on nonmetallic substrates which have been reported, the major enhancement mechanism occurred through charge-transfer enhancement.[24–26] A lack of SERS substrate generally limits the breadth of practical applications for SERS. Here, for the first time, we report the flower-shaped palladium iodide nanomaterials for use as SERS substrates. With regard to the trace detecting agent, we selected MG as the probe molecule, which was banned for use in aquaculture and the food industry due to its mutagenic and teratogenic effects to humans.[27] To illustrate the detection power of this system, we prepared MG aqueous solutions of different concentrations ranging from 1.0×10^{-4} M to 1.0×10^{-8} M. The corresponding Raman spectra of MG molecules enhanced by the flower-shaped PdI_2 materials/Si substrate were obtained. With respect to the positions of the peaks coming from the MG molecule, detailed assignments are shown in Table 1. The SERS substrate gave well-resolved Raman spectra of MG solutions, as shown in Fig. 7a–7d, which showed enhanced Raman peaks with the same Raman shift but different intensities. Obviously, the smaller the concentration of the MG solutions, the lower the intensity of the typical Raman scattering bands. Fig. 7e shows the Raman spectra of MG (1.0×10^{-4} M) on the pure Si substrate without PdI_2, the corresponding signal position was the same as the enhanced signal because of the higher concentration. However, the SERS of MG at a concentration of 1.0×10^{-8} M was not displayed (in Fig. 7) due to the poor signal to noise ratio. The detection power using PdI_2 nanomaterials as substrate could reach 1.0×10^{-7} M at the setting parameters. All the data were repeated multiple times at random spots and all of them showed significant Raman signals of MG at setting parameters. It is reasonable to expect that the as-produced PdI_2 nanomaterials could have a bright future in detecting contaminated food samples.

Table 1 Raman shift (cm^{-1}) and assignments of the bands of MG

Raman shift/cm^{-1}	band assignment
1298.23, 1485.87	benzene ring C–C stretching
1592.22, 1620.53	benzene ring C–C stretching
1373.29, 1396.93	*N*-phenyl stretching
1179.03	in-plane vibrations of ring C–H
1220.57	C–H rocking
916.54	ring skeletal vibration of radical orientation
803.75	out-of-plane vibrations of ring C–H

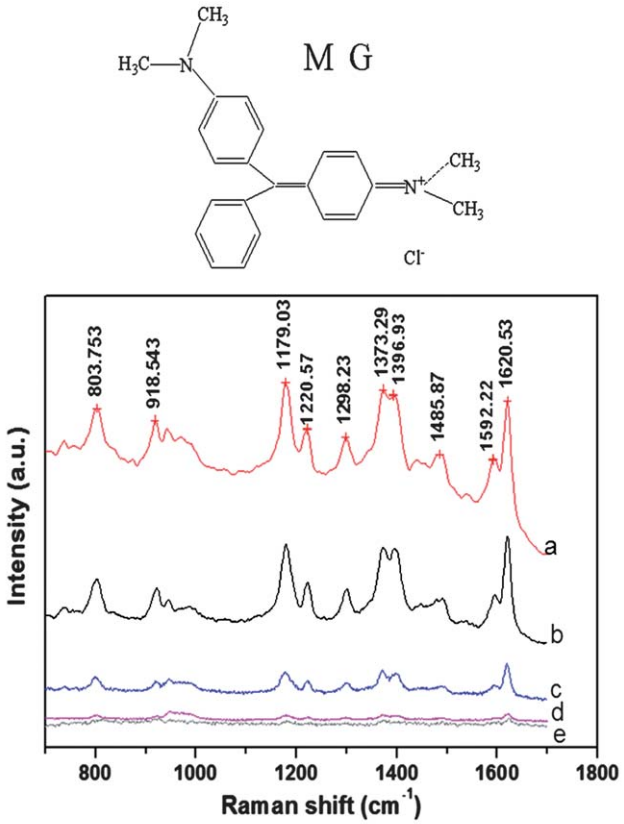

Fig. 7 The structural formula of malachite green (MG) and SERS of MG at different concentrations, (a) 1.0×10^{-4} M MG absorbed on flower-shaped PdI_2/Si substrate, (b) 1.0×10^{-5} M MG absorbed on flower-shaped PdI_2/Si substrate, (c) 1.0×10^{-6} M MG absorbed on flower-shaped PdI_2/Si substrate, (d) 1.0×10^{-7} M MG absorbed on flower-shaped PdI_2/Si substrate, (e) MG (1.0×10^{-4} M) on the pure Si substrate without PdI_2, all the acquisition times were 10 s, performed twice.

4. Conclusions

In summary, here, we demonstrated a simple, rapid and high yielding synthetic route to prepare flower-shaped PdI_2 nanomaterials. These flower-shaped PdI_2 nanoparticles possess preferential growth of nano-petals with radial [110] directions. This unique architecture made PdI_2 nanomaterials a good candidate for remarkable Raman signal detection. Tested with MG as the probe molecule, the sensitivity of the detection to MG could reach an order of 10^{-7} M. The flower-shaped PdI_2 nanoparticles thus showed great potential applications for SERS. This kind of SERS substrate composed of as-produced nanostructures possess the advantages of easy preparation, good reproducibility and high sensitivity. Consequently, the flower-shaped PdI_2 nanomaterials would have a bright future in detecting contaminated food samples.

Acknowledgements

This project was financially supported by the National Basic Research Program of China (2010CB934700), National Natural Science Foundation of China (50725208 & 20973019) as well as by Specialized Research Fund for the Doctoral Program of Higher Education (20091102110035).

References

1 M. M. Mañas and R. Pleixats, *Acc. Chem. Res.*, 2003, **36**, 638.
2 D. Astruc, *Inorg. Chem.*, 2007, **46**, 1884.
3 S. U. Son, Y. Jang, J. Park, H. B. Na, H. M. Park, H. J. Yun, J. Lee and T. Hyeon, *J. Am. Chem. Soc.*, 2004, **126**, 5026.
4 E. C. Walter, F. Favier and R. M. Penner, *Anal. Chem.*, 2002, **74**, 1546.
5 F. Yang, D. K. Taggart and R. M. Penner, *Nano Lett.*, 2009, **9**, 2177.
6 V. Bérubé, G. Radtke, M. Dresselhaus and G. Chen, *Int. J. Energy Res.*, 2007, **31**, 637.
7 Y. Nishihata, J. Mizuki, T. Akao, H. Tanaka, M. Uenishi, M. Klmura, T. Okamoto and N. Hamada, *Nature*, 2002, **418**, 164.
8 Y. Xiong, J. M. McLellan, J. Chen, Y. Yin, Z. Y. Li and Y. Xia, *J. Am. Chem. Soc.*, 2005, **127**, 17118.
9 M. E. Abdelsalam, S. Mahajan, P. N. Bartlett, J. J. Baumberg and A. E. Russell, *J. Am. Chem. Soc.*, 2007, **129**, 7399.
10 C. Xu, H. Wang, P. K. Shen and S. P. Jiang, *Adv. Mater.*, 2007, **19**, 4256.
11 C. Xiao, H. Ding, C. Shen, T. Yang, C. Hui and H. J. Gao, *J. Phys. Chem. C*, 2009, **113**, 13466.
12 P. Zhou, Z. Dai, M. Fang, X. Huang and J. Bao, *J. Phys. Chem. C*, 2007, **111**, 12609.
13 C. Li, R. Sato, M. Kanehara, H. Zeng, Y. Bando and T. Teranishi, *Angew. Chem., Int. Ed.*, 2009, **48**, 6883.
14 Y. H. Chen, H. H. Hung and M. H. Huang, *J. Am. Chem. Soc.*, 2009, **131**, 9114.
15 X. Huang and N. Zheng, *J. Am. Chem. Soc.*, 2009, **131**, 4602.
16 S. W. Kim, J. Park, Y. Jang, Y. Chung, S. Hwang, T. Hyeon and Y. W. Kim, *Nano Lett.*, 2003, **3**, 1289.
17 N. Tian, Z. Y. Zhou and S. G. Sun, *Chem. Commun.*, 2009, 1502.
18 B. A. Steinhoff, S. R. Fix and S. S. Stahl, *J. Am. Chem. Soc.*, 2002, **124**, 766.
19 C. Mousset, O. Provot, A. Hamze, J. Bignon, J. D. Brion and M. Alami, *Tetrahedron*, 2008, **64**, 4287.
20 B. Gabriele, G. Salerno, D. Brindisi, M. Costa and G. P. Chiusoli, *Org. Lett.*, 2000, **2**, 625.
21 R. S. Haya and D. B. Marshall, *Acta Mater.*, 2003, **51**, 5235.
22 X. M. Lin, Y. Cui, Y. H. Xu, B. Ren and Z. Q. Tian, *Anal. Bioanal. Chem.*, 2009, **394**, 1729.
23 B. Ren, G. K. Liu, X. B. Lian, Z. L. Yang and Z. Q. Tian, *Anal. Bioanal. Chem.*, 2007, **388**, 29.
24 A. Musumeci, D. Gosztola, T. Schiller, N. M. Dimitrijevic, V. Mujica, D. Martin and T. Rajh, *J. Am. Chem. Soc.*, 2009, **131**, 6040.
25 X. Ling, L. Xie, Y. Fang, H. Xu, H. Zhang, J. Kong, M. S. Dresselhaus, J. Zhang and Z. Liu, *Nano Lett.*, 2010, **10**, 553.
26 Y. Wang, W. Ruan, J. Zhang, B. Yang, W. Xu, B. Zhao and J. R. Lombardi, *J. Raman Spectrosc.*, 2009, **40**, 1072.
27 S. Srivastava, R. Sinha and D. Roya, *Aquat. Toxicol.*, 2004, **66**, 319.